HHS Public Access

Author manuscript

J Vasc Interv Radiol. Author manuscript; available in PMC 2017 March 01.

Published in final edited form as:

J Vasc Interv Radiol. 2016 March ; 27(3): 426–432.e1. doi:10.1016/j.jvir.2015.09.014.

In Vitro Capture of Small Ferrous Particles with a Magnetic Filtration Device Designed for Intravascular Use with Intraarterial Chemotherapy: Proof-of-Concept Study

Marc C. Mabray, MD, **Prasheel Lillaney, PhD**, **Chia-Hung Sze, MS**, **Aaron D. Losey, MD**, **Jeffrey Yang, BS**, **Sravani Kondapavulur, BS**, **Derek Liu, BS**, **Maythem Saeed, DVM, PhD**, **Anand Patel, MD**, **Daniel Cooke, MD**, **Young-Wook Jun, PhD**, **Ivan El-Sayed, MD**, **Mark Wilson, MD**, and **Steven W. Hetts, MD**

Departments of Radiology and Biomedical Imaging (M.C.M., P.L., C.H.S., A.D.L., J.Y., M.S., A.P., D.C., M.W., S.W.H.) and Otolaryngology–Head and Neck Surgery (I.E.-S.), University of California, San Francisco, San Francisco; and Department of Bioengineering (S.K., D.L.), University of California, Berkeley, Berkeley, California

Abstract

Purpose—To establish that a magnetic device designed for intravascular use can bind small iron particles in physiologic flow models.

Materials and Methods—Uncoated iron oxide particles 50–100 nm and 1–5 μm in size were tested in a water flow chamber over a period of 10 minutes without a magnet (ie, control) and with large and small prototype magnets. These same particles and 1-μm carboxylic acid–coated iron oxide beads were likewise tested in a serum flow chamber model without a magnet (ie, control) and with the small prototype magnet.

Results—Particles were successfully captured from solution. Particle concentrations in solution decreased in all experiments ($P < .05$ vs matched control runs). At 10 minutes, concentrations were 98% (50–100-nm particles in water with a large magnet), 97% (50–100-nm particles in water with a small magnet), 99% (1–5-μm particles in water with a large magnet), 99% (1–5-μm particles in water with a small magnet), 95% (50–100-nm particles in serum with a small magnet), 92% (1–5-μm particles in serum with a small magnet), and 75% (1-μm coated beads in serum with a small magnet) lower compared with matched control runs.

Address correspondence to M.C.M., Department of Radiology and Biomedical Imaging, University of California, San Francisco, 505 Parnassus Ave., M391, San Francisco CA, 94143; marc.mabray@ucsf.edu.

From the SIR 2015 Annual Meeting.

M.C.M. and P.L. have magnetic filtration device patents pending. C.H.S. a paid employee of ChemoFilter (Berkeley, California) outside the submitted work. A.P. and M.W. received personal fees and nonfinancial support from Penumbra (Alameda, California) outside the submitted work and hold patent PCT/US2013/076159 licensed to Penumbra. I.E.-S. has a patent pending for gold nanorods for photothermal therapy and optical diagnosis of cancer. S.W.H. received personal fees from Medina Medical (Menlo Park, California), personal fees and nonfinancial support from ChemoFilter, personal fees from Silk Road Medical (Sunnyvale, California), grants from Stryker Neurovascular (Fremont, California), and grants from MicroVention and Terumo (Somerset, New Jersey) outside the submitted work, and has a patent pending on related technology. None of the other authors have identified a conflict of interest.

Conclusions—This study demonstrates the concept of magnetic capture of small iron oxide particles in physiologic flow models by using a small wire-mounted magnetic filter designed for intravascular use.

Innovative ideas to potentially alter the manner in which intraarterial chemotherapy (IAC) is administered have included the use of drug-eluting beads, extracorporeal filtration, and, in recent preclinical studies, an ionic resin–based filter (1–6). An intravascular magnetic device could potentially be used to selectively remove a magnetic targeted carrier therapeutic agent without the need for extracorporeal filtration/perfusion or nonselective ionic binding mechanisms. In the present study, we explore the in vitro feasibility of such a concept, testing a magnetic device to remove iron oxide particles from solution.

Small magnetic iron oxide particles can be bound to therapeutic agents such as doxorubicin and used in IAC or transarterial chemoembolization as an oncologic treatment like standard agents while offering the distinct abilities to be manipulated by a magnetic field and tracked by magnetic resonance imaging (7–15). Previous studies that used a magnetic targeted carrier bound to doxorubicin (MTC-DOX) showed that an external magnet placed over the liver of the patient could influence MTC-DOX distribution in patients with hepatocellular carcinoma (14,16). MTC-DOX was estimated to release 25% of the bound drug into human plasma over a period of 3 hours, but numerous different types of magnetic iron oxide particles have been bound to doxorubicin, with different affinities, stabilities, sizes, and behaviors in various microenvironments depending on the characteristics of the particles (7,8,10,15,17,18). Other agents and classes of medications, including thrombolytic agents, have also been bound to iron oxide particles and could potentially also be used with the technology developed in this investigation (7,8,19–21).

The magnetic properties of MTC-DOX or similar agents could potentially be used to remove the agents from the circulation, thereby decreasing systemic concentrations and toxicity and allowing dose escalation to provide a better therapeutic effect. The purpose of this proof-of-concept study was to establish that a magnetic intravascular device could bind small iron oxide particles in in vitro flow models. The hypothesis was that a small magnetic device could be designed and constructed for intravascular use and could capture iron oxide particles in vitro.

MATERIALS AND METHODS

Magnetic Devices

An initial large prototype magnetic device was empirically constructed for initial in vitro experiments. This larger device consisted of 20 individual neodymium ring magnets (N52 grade, 12.5-mm outer diameter, 3-mm inner diameter, 3-mm length, estimated surface field of 3,400 G/0.34 T; K&J Magnetics, Pipersville, Pennsylvania) placed on a bolt in “cow magnet” configuration with like polarities facing and repelling each other and secured with a bolt (Fig 1). This larger device was used for initial flow chamber testing.

A second smaller device was constructed with size constraints to allow for eventual percutaneous introduction into the venous system (Fig 1). This device was constructed on a

0.014-inch-diameter guide wire (Transend 300 ES; Boston Scientific, Marlborough, Massachusetts) by using 15 neodymium ring magnets (N52 grade, 5-mm length, 4-mm outer diameter, 1-mm inner diameter, estimated surface field of 500 G/0.05 T; SuperMagnetMan Magnetics, Pelham, Alabama). These smaller magnets were placed on the 0.014-inch guide wire with like polarities facing and repelling each other. Approximately 3 mm of space was left between the repelling magnets to increase coverage and because the repelling magnetic forces could not be overcome easily. The proximal- and distal-end magnets were secured in position with layers of tape built up just beyond the magnet, heated shrink-wrap applied over the tape, and a small amount of glue adhesive. The overall length of the magnetic portion of this device was 11.5 cm. This device was introduced into an 18-F sheath with a one-way valve by using an introducer (Cook, Indianapolis, Indiana).

Particles

For initial testing, 50–100-nm uncoated iron oxide particles in powder form (iron[II,III] oxide; Sigma-Aldrich, St. Louis, Missouri) and 1–5-μm uncoated iron oxide particles in powder form (iron[II,III] oxide; Sigma-Aldrich) were selected. To evaluate more uniform coated particles in solution, iron oxide beads approximately 1 μm in size (800 nm by dynamic light scattering) with a COOH (carboxylic acid) coat in solution were selected (26.5% by weight iron[II,III] oxide; ProMag 1 Series COOH; Bangs Laboratories, Fishers, Indiana). Standard concentrations of each type of particle in deionized water were used to make standard curves by using absorbance spectrophotometry (U2810 Spectrophotometer; Hitachi Digilab, Tokyo, Japan). To assess if the uncoated powder particles clumped together when put into solution, particle size in solution in water was evaluated with dynamic light scattering (Zetasizer Nano ZS90; Malvern Instruments, Malvern, United Kingdom).

In Vitro Testing in a Water Flow Chamber

The 50–100-nm and 1–5-μm uncoated iron oxide particles were initially tested in a water flow chamber. A total of 250 mg of particles were placed in 500 mL of water (0.5 mg/mL) in a closed circuit flow model. The flow model consisted of a 1,000-mL glass reservoir with 1.2-cm polyvinyl chloride tubing (Masterflex, Vernon Hills, Illinois) and a peristaltic pump (Masterflex). The particles in the reservoir were continuously mixed pneumatically with a 6-mL syringe, and the fluid was continuously cycled through the tubing at a rate of 750 mL/min to approximate hepatic venous flow. The system was allowed to equilibrate in this manner for 5 minutes. A 3-mL sample was taken from the reservoir at time 0 as the magnetic device was inserted into the tubing, and then 3-mL samples were taken at 1, 3, 5, and 10 minutes. The pump was then stopped and the magnet removed.

Visual clearing of the solution over time was assessed. The magnetic device was visually assessed for adherent iron particles. Light microscopy was then performed to visualize adherent iron oxide particles. Iron oxide particle concentration remaining in solution was quantified in milligrams per milliliter by absorbance spectrophotometry with comparison versus the appropriate standard curve. This process was performed three times as control without a magnet, three times with the large magnet, and three times with the small wire-based magnet for the 50–100-nm uncoated iron oxide particles and for the 1–5-μm uncoated iron oxide particles (18 total runs, six of which are controls).

In Vitro Testing in Serum Flow Chamber

Following in vitro water testing, in vitro testing in serum was performed to provide a more physiologically realistic scenario given the increased viscosity of serum. The same flow chamber model used for initial testing in water was now used with pig serum (Fig 2) in the reservoir and with the methods described earlier. Before absorbance spectrophotometry, a large magnet (five N52 disk magnets stuck together, each with a 19-mm outer diameter and 5 mm thick; K&J Magnetics) was applied to the serum sample and used to pull the particles to the bottom of the sample tube. The serum was then removed from the tube, and the particles were washed with water. That water was then removed, and the particles were suspended in 3 mL of water for absorbance spectrophotometry. Three runs were performed as controls and three runs were performed with the smaller wire-based magnetic device for the 50–100-nm uncoated iron oxide particles, the 1–5-μm uncoated iron oxide particles, and the 1-μm COOH-coated iron oxide beads (18 total runs, nine of which are controls).

Statistical Analysis

Statistical analysis was performed with MedCalc software (version 14.8.1; MedCalc, Ostend, Belgium) for Windows (Microsoft, Redmond, Washington). As there were slight variations in starting concentrations at time 0 for flow chamber runs, the concentrations were normalized to time 0 for each run and expressed as proportional concentrations (ie, proportion remaining in solution vs time 0). The mean and standard deviation were calculated at each time point for each set of three runs, and the proportional concentrations were plotted against time. The time-weighted mean proportional concentration (area under the curve divided by time) was used as a summary statistic of each concentration curve set, and the curves were compared with a two-tailed *t* test for sets of two runs (serum experiments) and one-way analysis of variance with Student–Newman–Keuls pairwise comparisons for sets of three runs (water experiments). A P value < .05 was considered statistically significant.

RESULTS

Particle Characterization

The initially tested 50–100-nm and 1–5-μm uncoated iron oxide particles in powder form exhibited clumping visually when placed into solution. The 50–100-nm particles measured 1,354 nm (1.354 μm) by dynamic light scattering when in solution, much larger than their reported size from the manufacturer, suggesting aggregation/clumping in solution. The 1–5-μm particles measured 1,292 nm (1.292 μm) by dynamic light scattering when in solution, although the upper limit of size characterization by this method is approximately 10 μm. Much larger particle aggregates were visible in the solution and were likely not measured. The approximately 1-μm COOH-coated iron oxide beads in solution measured 993 nm by dynamic light scattering, and there was no visible clumping in solution.

In Vitro Testing in a Water Flow Chamber

The 50–100-nm uncoated iron oxide particles were captured from solution by the larger magnetic filtration device (Fig 1b) and by the smaller magnetic filtration device (Fig 1c)

designed for intravascular use. This was apparent through visual clearing of the solution in the reservoir as it passed by the magnetic filtration device, and in consecutive samples. Following the experiment, iron oxide particles were seen on the magnetic device on visual inspection and by light microscopy. The concentration of iron particles in solution decreased over time in the experiments with the larger prototype magnetic filter present and in the experiments with the smaller magnetic filter present (Table 1 and Fig E1 [available online at www.jvir.org]). At 10 minutes, the concentration remaining in solution was 98% lower for large magnet runs and 97% lower for small magnet runs compared with control runs. This was validated statistically: concentration curves were significantly different (analysis of variance, $F = 834.991$, $P < .001$) for the large magnet runs ($P < .05$) and for the small magnet runs ($P < .05$) compared with control runs.

The 1–5-μm uncoated iron oxide particles were also captured from solution by the larger magnetic filtration device and the smaller magnetic filtration device with similar results (Table 1 and Fig E1 [available online at www.jvir.org]). Concentrations decreased over time in experimental runs with the magnets compared with control runs. At 10 minutes, the concentrations remaining in solution were 99% lower for large magnet runs and 99% lower for small magnet runs compared with control runs. Concentration curves were significantly different (analysis of variance, $F = 79.445$, $P < .001$) for the large magnet runs ($P < .05$) and for the small magnet runs ($P < .05$) compared with control runs.

In Vitro Testing in Serum Flow Chamber

The 50–100-nm and 1–5-μm uncoated iron oxide particles were also effectively captured from serum in the flow chamber by the smaller magnetic filtration device designed for intravascular use, as evidenced by decreasing concentrations of particles in solution compared with control runs (Fig 3 and Table 2). At 10 minutes, the concentrations remaining in solution were 95% lower for the 50–100-nm particle runs and 92% lower for the 1–5-μm particle runs compared with their control runs. Concentration curves were significantly different for 50–100-nm particles ($P = .002$) and for 1–5-μm particles ($P = .004$) with the small magnet compared with the matched serum control runs.

The experiments with the COOH-coated 1-μm beads validated the results with uncoated particles, as the magnetic forces of these particles would be less (as they are only 26.5% iron oxide by weight), but clumping and heterogeneity would also be expected to be less. These COOH-coated beads were also effectively removed from the serum flow model with the use of the smaller magnetic filtration device, with decreasing concentrations of particles remaining in solution (Fig 3 and Table 2). At 10 minutes, the concentration remaining in solution was 75% lower for the magnet runs compared with the control runs. Concentration curves were significantly different ($P = .0164$) for the runs with the smaller magnetic device than for the matched control runs.

DISCUSSION

The present study demonstrates the concept of magnetic filtration of magnetic particles in physiologic flow models. An initial larger magnetic filtration device (12.5-mm diameter) was first constructed and tested in a flow model with water to help prove the concept. A

smaller wire-based magnetic filtration device intended for endovascular use (4-mm diameter) was then modeled, constructed, and tested in flow models with water and under more physiologic conditions with serum. Concentrations of particles in solution were significantly decreased in the presence of the magnetic devices in all experiments compared with their matched controls, demonstrating in vitro capture.

This concept could potentially be combined in the future with existing or new therapeutic agents bound to magnetic carriers to create a novel paradigm for locoregional therapy, allowing intraarterial infusion of high concentrations of iron-bound therapeutic agents with magnetic sequestration of excess particles from the venous system. Other filtration ideas proposed for IAC have included extracorporeal filtration and an ionic resin–based filter, which require physiology-altering extracorporeal blood flow or ionic mechanisms that may be plagued by nonspecific ionic binding to normal ions present in the blood (1–3,6). The concept presented here would offer an alternative means of filtration with the magnetic attraction of iron oxide particles to a wire-based intravascular device. Magnetic therapeutic agents are an area of active research, and numerous particles have been developed that are tailored for different uses (7,8,10,15,17–21). Magnetic manipulation of iron particles has been performed in the setting of IAC to help localize particles with an external magnet and also with alternating magnetic fields to create local hyperthermia in tumors (ie, magnetic fluid hyperthermia) and augment thrombolysis (7–10,14–16,19,20,22–25). The concept proposed here is to use magnetism for the purposes of intravascular filtration.

This is a proof-of-concept study, and, as such, there are a number of limitations. Magnetic filter design was largely empiric, based on the theoretic concept, size constraints for in vivo use, and commercially available materials. Future designs could incorporate magnetic field modeling along with computational fluid dynamics to optimize device function. The particles chosen for experiments were initially selected for cost effectiveness, availability, and safety. In the future, magnetic particles already bound to chemotherapeutic or other therapeutic agents could be used to better simulate therapeutic interventions. This line of research is therefore dependent on particle experts continuing to develop and refine therapeutic particles with appropriate stability, affinity, and behavior for use with a system such as the one described here (7,8,10,15,17,18). Clumping of the dry uncoated particles when placed into solution caused them to have a larger effective size than reported by the manufacturer (> 1 μm for the 50–100-nm particles and likely >10 μm but beyond the limits of detection by dynamic light scattering for the 1–5-μm particles). Clumping, along with heterogeneous mixing and layering in the flow chamber and stochastic error, likely contributed to the inconsistent measurements in the control experiments. The third type of particle tested was a COOH-coated bead, which was used to address concerns regarding particle clumping and heterogeneity that arose with the use of the less expensive uncoated particles. This study therefore tested particles in the micron range of sizes, and extrapolation to true nanoparticle-scaled particles is limited; future studies may test additional nanometer-scale particles. Definitive animal experiments are needed for further evaluation, which would include biodistribution studies and IAC in a liver tumor model with the use of magnetic therapeutic agents such as MTC-DOX.

In conclusion, the present study has demonstrated the concept of magnetic capture of small magnetic iron oxide particles in vitro by using a small wire-based magnetic filter designed for intravascular use. This concept and device could potentially be applied in the future to a variety of oncologic and nononcologic locoregional therapies throughout the body.

Supplementary Material

Refer to Web version on PubMed Central for supplementary material.

Acknowledgments

The authors thank Thomas Haas for assistance with particle characterization and expertise and Korrie Mabray for assistance with device design. This study was supported by National Institutes of Health Grants 5R01EB012031 (S.W.H.), 1R41CA183327 (A.P.), 1R01CA194533 (S.W.H.), 5T32EB001631-10 (M.C.M.; Thomas Link, principal investigator), and R25EB013068 (S.K., D.L.; Amy Herr, principal investigator).

ABBREVIATIONS

IAC	intraarterial chemotherapy
MTC-DOX	magnetic targeted carrier bound to doxorubicin

References

1. Fuhrman GM, Cromeens DM, Newman RA, et al. Hepatic arterial infusion of verapamil and doxorubicin with complete hepatic venous isolation and extracorporeal chemofiltration: pharmacological evaluation of reduction in systemic drug exposure and assessment of hepatic toxicity. Surg Oncol. 1994; 3:17–25. [PubMed: 8186867]
2. Curley SA, Newman RA, Dougherty TB, et al. Complete hepatic venous isolation and extracorporeal chemofiltration as treatment for human hepatocellular carcinoma: a phase I study. Ann Surg Oncol. 1994; 1:389–399. [PubMed: 7850540]
3. Curley SA, Byrd DR, Newman RA, et al. Reduction of systemic drug exposure after hepatic arterial infusion of doxorubicin with complete hepatic venous isolation and extracorporeal chemofiltration. Surgery. 1993; 114:579–585. [PubMed: 8367814]
4. Song MJ, Chun HJ, Song do S, et al. Comparative study between doxorubicin-eluting beads and conventional transarterial chemoembolization for treatment of hepatocellular carcinoma. J Hepatol. 2012; 57:1244–1250. [PubMed: 22824821]
5. Lammer J, Malagari K, Vogl T, et al. Prospective randomized study of doxorubicin-eluting-bead embolization in the treatment of hepatocellular carcinoma: results of the PRECISION V study. Cardiovasc Intervent Radiol. 2010; 33:41–52. [PubMed: 19908093]
6. Patel AS, Saeed M, Yee EJ, et al. Development and validation of endovascular chemotherapy filter device for removing high-dose doxorubicin: preclinical study. J Med Device. 2014; 8:0410081–0410088. [PubMed: 25653735]
7. Weinstein JS, Varallyay CG, Dosa E, et al. Superparamagnetic iron oxide nanoparticles: diagnostic magnetic resonance imaging and potential therapeutic applications in neurooncology and central nervous system inflammatory pathologies, a review. J Cereb Blood Flow Metab. 2010; 30:15–35. [PubMed: 19756021]
8. Alexiou C, Jurgons R, Seliger C, Brunke O, Iro H, Odenbach S. Delivery of superparamagnetic nanoparticles for local chemotherapy after intra-arterial infusion and magnetic drug targeting. Anticancer Res. 2007; 27:2019–2022. [PubMed: 17649815]
9. Mouli SK, Tyler P, McDevitt JL, et al. Image-guided local delivery strategies enhance therapeutic nanoparticle uptake in solid tumors. ACS Nano. 2013; 7:7724–7733. [PubMed: 23952712]

10. Wang Y, Wei X, Zhang C, Zhang F, Liang W. Nanoparticle delivery strategies to target doxorubicin to tumor cells and reduce side effects. Ther Deliv. 2010; 1:273–287. [PubMed: 22816133]
11. El-Sayed IH. Nanotechnology in head and neck cancer: the race is on. Curr Oncol Rep. 2010; 12:121–128. [PubMed: 20425597]
12. Echevarria-Uraga JJ, Garcia-Alonso I, Plazaola F, et al. Study of the intra-arterial distribution of Fe(3)O(4) nanoparticles in a model of colorectal neoplasm induced in rat liver by MRI and spectrometry. Int J Nanomedicine. 2012; 7:2399–2410. [PubMed: 22661893]
13. Lyer S, Tietze R, Jurgons R, et al. Visualisation of tumour regression after local chemotherapy with magnetic nanoparticles–a pilot study. Anticancer Res. 2010; 30:1553–1557. [PubMed: 20592340]
14. Wilson MW, Kerlan RK Jr, Fidelman NA, et al. Hepatocellular carcinoma: regional therapy with a magnetic targeted carrier bound to doxorubicin in a dual MR imaging/conventional angiography suite–initial experience with four patients. Radiology. 2004; 230:287–293. [PubMed: 14695402]
15. Munnier E, Cohen-Jonathan S, Linassier C, et al. Novel method of doxorubicin-SPION reversible association for magnetic drug targeting. Int J Pharm. 2008; 363:170–176. [PubMed: 18687392]
16. Goodwin SC, Bittner CA, Peterson CL, Wong G. Single-dose toxicity study of hepatic intra-arterial infusion of doxorubicin coupled to a novel magnetically targeted drug carrier. Toxicol Sci. 2001; 60:177–183. [PubMed: 11222884]
17. Tacar O, Sriamornsak P, Dass CR. Doxorubicin: an update on anticancer molecular action, toxicity and novel drug delivery systems. J Pharm Pharmacol. 2013; 65:157–170. [PubMed: 23278683]
18. Rudge SR, Kurtz TL, Vessely CR, Catterall LG, Williamson DL. Preparation, characterization, and performance of magnetic iron-carbon composite microparticles for chemotherapy. Biomaterials. 2000; 21:1411–1420. [PubMed: 10872770]
19. Chen JP, Yang PC, Ma YH, Tu SJ, Lu YJ. Targeted delivery of tissue plasminogen activator by binding to silica-coated magnetic nanoparticle. Int J Nanomedicine. 2012; 7:5137–5149. [PubMed: 23055726]
20. Voros E, Cho M, Ramirez M, et al. TPA immobilization on iron oxide nanocubes and localized magnetic hyperthermia accelerate blood clot lysis. Adv Funct Mater. 2015; 25:1709–1718.
21. Kohler N, Sun C, Fichtenholtz A, Gunn J, Fang C, Zhang M. Methotrexate-immobilized poly(ethylene glycol) magnetic nanoparticles for MR imaging and drug delivery. Small. 2006; 2:785–792. [PubMed: 17193123]
22. Gneveckow U, Jordan A, Scholz R, et al. Description and characterization of the novel hyperthermia- and thermoablation-system MFH 300F for clinical magnetic fluid hyperthermia. Med Phys. 2004; 31:1444–1451. [PubMed: 15259647]
23. Wust P, Gneveckow U, Johannsen M, et al. Magnetic nanoparticles for interstitial thermotherapy–feasibility, tolerance and achieved temperatures. Int J Hyperthermia. 2006; 22:673–685. [PubMed: 17390997]
24. Johannsen M, Gneveckow U, Thiesen B, et al. Thermotherapy of prostate cancer using magnetic nanoparticles: feasibility, imaging, and three-dimensional temperature distribution. Eur Urol. 2007; 52:1653–1661. [PubMed: 17125906]
25. Maier-Hauff K, Rothe R, Scholz R, et al. Intracranial thermotherapy using magnetic nanoparticles combined with external beam radiotherapy: results of a feasibility study on patients with glioblastoma multiforme. J Neurooncol. 2007; 81:53–60. [PubMed: 16773216]

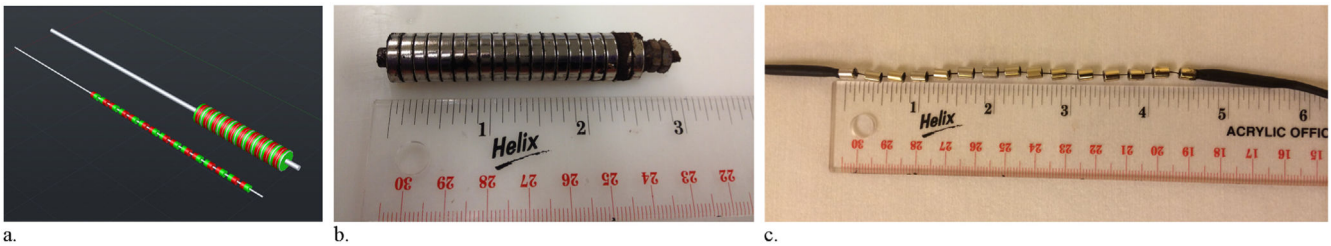

a. b. c.

Figure 1.

Magnetic filtration devices. **(a)** Computer-aided design of the small and large magnetic filter devices demonstrates the alternating polarity design (ie, like poles facing and repelling each other). **(b)** The large magnetic filtration device and **(c)** the smaller wire-based magnetic filtration device.

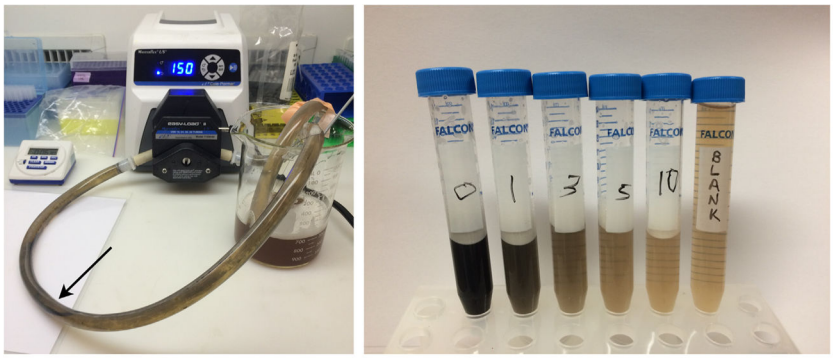

a. b.

Figure 2.

Flow chamber experiments. **(a)** The smaller magnetic filtration device in the flow chamber during a serum experiment (arrow). **(b)** Samples were taken at times 0, 1, 3, 5, and 10 minutes during a serum flow chamber experiment and compared with blank serum. Note the visual clearing of the serum over time as the concentration of particles decreases.

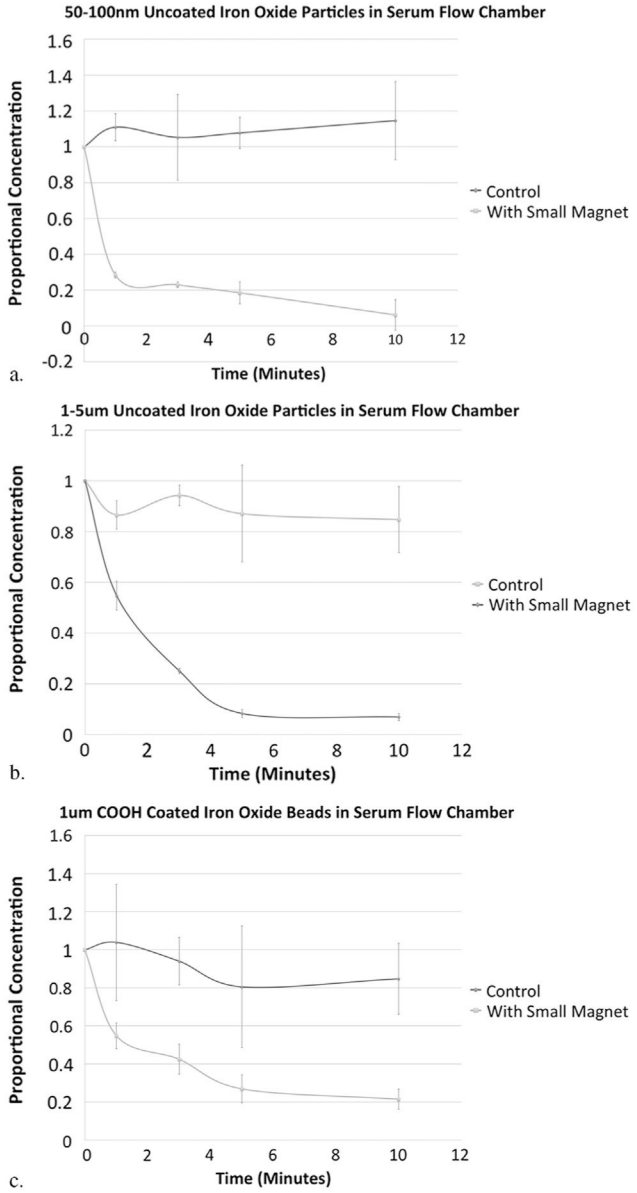

Figure 3.

Concentration curves (ie, proportion remaining in solution compared with time 0 for each run, with error bars representing standard deviation) from flow chamber experiments and corresponding control experiments for 50–100-nm uncoated iron oxide particles in serum **(a)**, 1–5-μm uncoated iron oxide particles in serum **(b)**, and 1-μm COOH-coated iron oxide beads in serum **(c)**. The concentration decreased over time in the experiments with the large and small magnetic filtration devices compared with controls. The inconsistency in measurements during the control experiments may in part reflect heterogeneous mixing and clumping of the uncoated particles in solution.

Table 1

Results of In Vitro Water Flow Chamber Experiments

Experiment	0 min	1 min	3 min	5 min	10 min	Time-Weighted Average	*P* Value*
50–100-nm							
Control	1	0.899 ± 0.068	1.119 ± 0.254	1.009 ± 0.022	1.056 ± 0.056	1.026 ± 0.038 (0.930–1.121)	
Large magnet	1	0.173 ± 0.072	0.032 ± 0.014	0.017 ± 0.010	0.012 ± 0.006	0.092 ± 0.015 (0.054–0.129)	< .05
Small magnet	1	0.334 ± 0.099	0.137 ± 0.054	0.065 ± 0.030	0.033 ± 0.009	0.158 ± 0.035 (0.072–0.245)	< .05
1–5-μm							
Control	1	0.886 ± 0.058	1.086 ± 0.243	0.980 ± 0.197	1.004 ± 0.176	0.994 ± 0.169 (0.575–1.414)	
Large magnet	1	0.240 ± 0.036	0.081 ± 0.049	0.018 ± 0.009	0.011 ± 0.014	0.111 ± 0.010 (0.085–0.137)	< .05
Small magnet	1	0.329 ± 0.032	0.097 ± 0.016	0.037 ± 0.004	0.010 ± 0.006	0.134 ± 0.009 (0.112–0.156)	< .05

Note–Values presented as mean ± standard deviation. Values in parentheses are 95% confidence intervals.

* Concentrations in water were lower in experimental runs with the magnet compared with matched controls by analysis of variance with Student–Newman–Keuls pairwise comparisons.

Table 2

Results of In Vitro Serum Flow Chamber Experiments

Experiment	0 min	1 min	3 min	5 min	10 min	Time-Weighted Average	*P* Value*
50–100 nm uncoated iron oxide particles							
Control	1	1.110 ± 0.075	1.052 ± 0.239	1.078 ± 0.088	1.146 ± 0.218	1.091 ± 0.106 (0.826–1.355)	
Small magnet	1	0.284 ± 0.017	0.230 ± 0.016	0.185 ± 0.062	0.062 ± 0.085	0.219 ± 0.042 (0.114–0.323)	< .05
1–5 μm uncoated iron oxide particles							
Control	1	0.866 ± 0.056	0.942 ± 0.041	0.871 ± 0.191	0.847 ± 0.131	0.885 ± 0.107 (0.619–1.151)	
Small magnet	1	0.547 ± 0.058	0.250 ± 0.011	0.083 ± 0.016	0.069 ± 0.014	0.228 ± 0.003 (0.220–0.237)	< .05
1–μm COOH-coated iron oxide beads							
Control	1	1.039 ± 0.305	0.939 ± 0.124	0.805 ± 0.320	0.847 ± 0.186	0.887 ± 0.225 (0.328–1.446)	
Small magnet	1	0.548 ± 0.067	0.424 ± 0.079	0.269 ± 0.074	0.215 ± 0.053	0.365 ± 0.033 (0.282–0.448)	< .05

Note–Values presented as mean ± standard deviation. Values in parentheses are 95% confidence intervals.

* Concentrations in serum were lower in experimental runs with the magnet compared to matched controls by *t* test.

J Vasc Interv Radiol. Author manuscript; available in PMC 2017 March 01.